METALLURGICAL AND CORROSION FEATURES OF FRICTION STIR WELDING OF AA5083-H111



P. Vilaça[1] **N. Pépe** **L. Quintino**

Technical University of Lisbon, Instituto Superior Técnico (Portugal)

E-mail[1]: pedro.vilaca@ist.utl.pt

ABSTRACT

Friction stir welding is a solid state joining process, which has been considered the most important development in the welding technology, in the last decade, especially in the joining of light alloys such as aluminium alloys. The increasing applications of these materials in industry give rise to significant development of this process in world scale. The material analysed in this work is the non-heat treatable aluminium alloy AA5083-H111, strain hardened with significant applications, e.g., shipbuilding and automotive industries. Metallurgical features are investigated, such as, the diffusion of initial precipitates and changes of grain size in the heat-affected zone and thermal-mechanically affected zone, resulting from the thermal-mechanical cycle of the friction stir welding process. The results allow to understand the mechanisms that determine the metallurgical changes in the weld bead. The metallographic analysis is compared with hardness tests developed in all zones of the welded joint, enabling conclusions about the mechanical resistance efficiency. The localization and form of corrosion initiation is also evaluated, as well as the influence of the chemical composition of the solid solution matrix of aluminium and secondary phases in the susceptibility to corrosion of parent material and weld bead.

IIW-Thesaurus keywords: *Friction stir welding; Friction welding; Metallurgy; Corrosion; Corrosion tests; Exfoliation; Intergranular corrosion; Hardness tests; Mechanical tests; Electron microscopes; Measuring instruments; Microscopes; Aluminium alloys; Light metals; Practical investigations; Reference lists.*

1 INTRODUCTION

The application of aluminium alloys is increasing in all industries due to its combination of properties of low weight, good mechanical resistance, and good corrosion resistance [1]. One of the industries where the application of aluminium is becoming more important is shipbuilding, which is one of the main means responsible for the transport of people and goods in the world [2, 3, 4]. The need for fast and less expensive ships demands the advantages of Friction Stir Welding (FSW) [2]. Typically, shipbuilding applies wrought aluminium alloys of series 5XXX and 6XXX [3, 4].

FSW is an autogenous solid state process, in which a rotating non-consumable cylindrical tool, with a somewhat complex shoulder and pin profile, is forced to transverse along the joint line producing the weld [5, 6, 7]. The high potential of FSW to perform joints with high quality, control, and repeatability in materials of low weldability, such as light alloys in general, and aluminum alloys in particular, extended the application field of welding construction allowing the application of new materials in product design [6, 7, 8].

The selection of the correct tool geometry, for the different types of joints, materials and thicknesses, is one of the most important parameters in the performance of FSW [9].

The transfer of FSW into industrial applications, such as shipbuilding, demands a detailed investigation about the influence of corrosion in the performance of both parent materials and welded joints. The main mechanisms of corrosion that have been evaluated in AA5XXX are intergranular corrosion and exfoliation. Work performed by other authors indicated that in FSW joints the

Doc. IIW-1746-06 (ex-doc. IX-2148-05) recommended for publication by Commission IX "Behaviour of metals subjected to welding".

Thermal-Mechanically Affected Zone (TMAZ) is where the corrosion effects are more significant [10, 11, 12].

In the present work metallurgical features are investigated and compared with hardness tests developed in all zones of the welded joint, enabling conclusions about the mechanical resistance efficiency. Also evaluated is the localization and form of corrosion initiation along with the influence of chemical composition of the solid solution matrix of aluminium and secondary phases in the susceptibility to corrosion of the parent material and weld bead.

The present report starts with the presentation of the experimental conditions and procedures, followed by the results obtained and the correspondent analysis. Finally, the conclusions are established.

2 EXPERIMENTAL DETAILS

2.1 Materials

The material used was AA5083-H111 rolled to a thickness of 4 mm. All the welds were performed in a butt joint arrangement. The chemical composition and mechanical properties are presented in Table 1.

2.2 Welding conditions

Preliminary studies for the development of FSW parameters of AA5083-H111 with 4 mm of thickness have been made [13]. Resulting from the mechanical resistance analysis, the best two groups of parameters have been selected and implemented during the present work.

All the welds were performed in the rolling direction in a conventional milling machine. The rotation speed was 1 120 rpm and the travel speed was 320 mm/min in all the welds. The tool used was a modular tool allowing a combination of different geometries of shoulders and pins, and also the continuous variation of the pin length.

Two different shoulder geometries were used with a cylindrical pin M5 threaded with 3 flats with a length of 3.9 mm. The different shoulder geometries investigated were the following:

– Smooth concave with 7° and an outer diameter of 15 mm. This shoulder was implemented with a tilt angle of 2°.

– Flat with 3 concentric striates of 2 mm depth and an outer diameter of 17 mm. This shoulder was implemented with a tilt angle of 1°.

2.3 Metallographic analysis

The metallographic analysis allows characterization of the influence of the welding process in the microstructure of the parent material. Distribution of the precipitates in the different zones of the weld and the changes of grain size resulting from the FSW process were investigated. The results obtained were then compared with hardness tests.

2.4 Intergranular corrosion

Intergranular corrosion tests following the ASTM G67 were performed on parent material and samples of the two different weld conditions. This standard procedure applies to the determination of the susceptibility to intergranular corrosion of AA5XXX, quantifying the mass loss after exposure to nitric acid (NAMLT Test) [14]. This test method consists of immerging test specimens in concentrated nitric acid at 30 °C for 24 h and determining the mass loss per unit area as a measure of susceptibility to intergranular corrosion. The objective of this test is to provide a quantitative measure of the susceptibility to intergranular corrosion of Al-Mg alloys. The nitric acid dissolves a second phase, an aluminium-magnesium intermetallic compound (βAl-Mg), in preference to the solid solution of magnesium in the aluminium matrix.

Samples 6 mm × 50 mm × 4 mm were prepared in the following stages:

(a) pickling, by immersing of samples in 5 % NaOH solution at 80 °C during 1 min,

(b) desmuting, by immersing of samples in HNO_3 at room temperature, during 30 s, and

(c) weighing the samples.

After immersing the samples in the solution test the mass loss was determined and the different results were analysed.

2.5 Exfoliation tests

Exfoliation corrosion tests following the ASTM G66 were performed on parent material and samples of the two different weld conditions. This standard practice applies to visual assessment of exfoliation corrosion susceptibility of AA5XXX (ASSET Test) [15]. Samples are immersed for 24 h at 65 ± 1 °C in a solution containing ammonium chloride, ammonium nitrate, ammonium tartrate, and hydrogen peroxide. This test method provides a reliable prediction of the exfoliation corrosion behaviour of Al-Mg alloys in marine environments.

Samples 40 mm × 100 mm × 4 mm were prepared in the following stages:

(a) pickling, by immersing of samples in 5 % NaOH solution at 80 °C during 1 min, and

Table 1 – Chemical composition and mechanical properties of AA5083-H111 plates

Elements	Si	Fe	Cu	Mn	Mg	Cr	Zn	Ti	Al
Chemical Composition	0.12	0.33	0.03	0.51	4.39	0.08	0.01	0.02	remain
Proof strength (MPa)		153	**Tensile strength (MPa)**			297	**Elongation [%]**		22

(b) desmuting, by immersing of samples in HNO_3 at room temperature, during 30 s.

After immersing the samples in the solution test a visual ranking was attributed by comparing the visual aspect of the surface with standard reference photographs.

2.6 Characterization of corrosion test samples

After the visual analysis, the morphology of corrosion of all samples resulting from the corrosion tests were analysed by Scanning Electron Microscopy (SEM).

3 ANALYSIS OF THE RESULTS

3.1 Metallographic analysis

The two different welding conditions were subjected to a detailed metallurgical analysis. In Figures 1 and 2, it is possible to analyse the different aspects of the macrographs, including some of the most relevant characteristics; e.g., relative location of the centre of the nugget, width of the nugget at the centre and at the root of the weld (Table 2). This last dimension is very relevant in the quality assessment of the FSW joints because defects located at the root of the bead are always important [8].

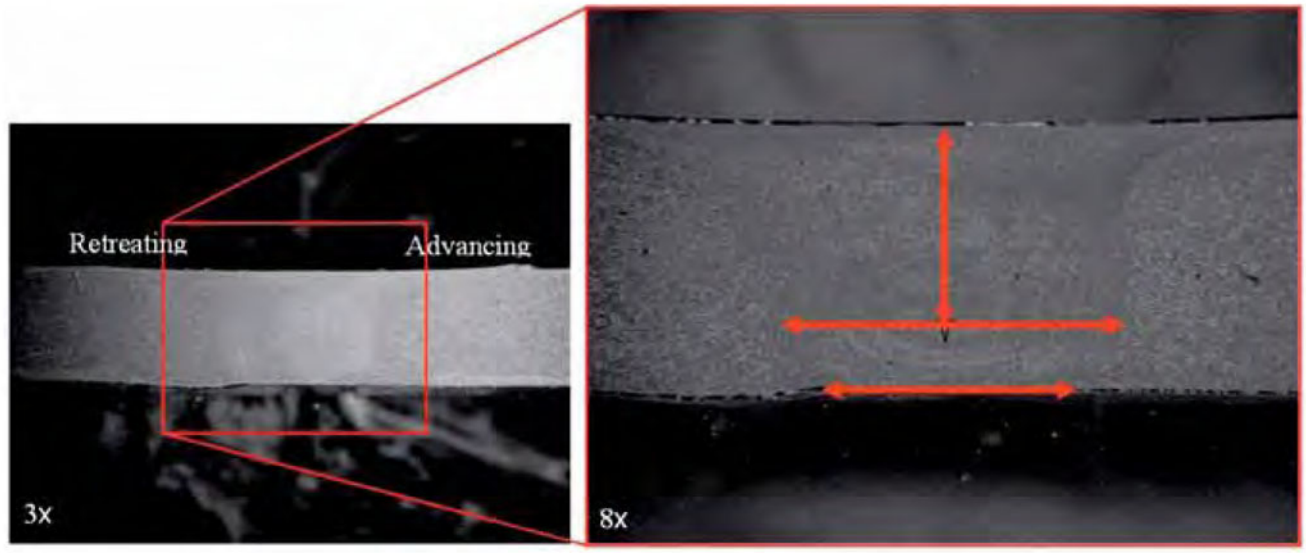

Figure 1 – Photomacrograph of FSW with smooth concave shoulder

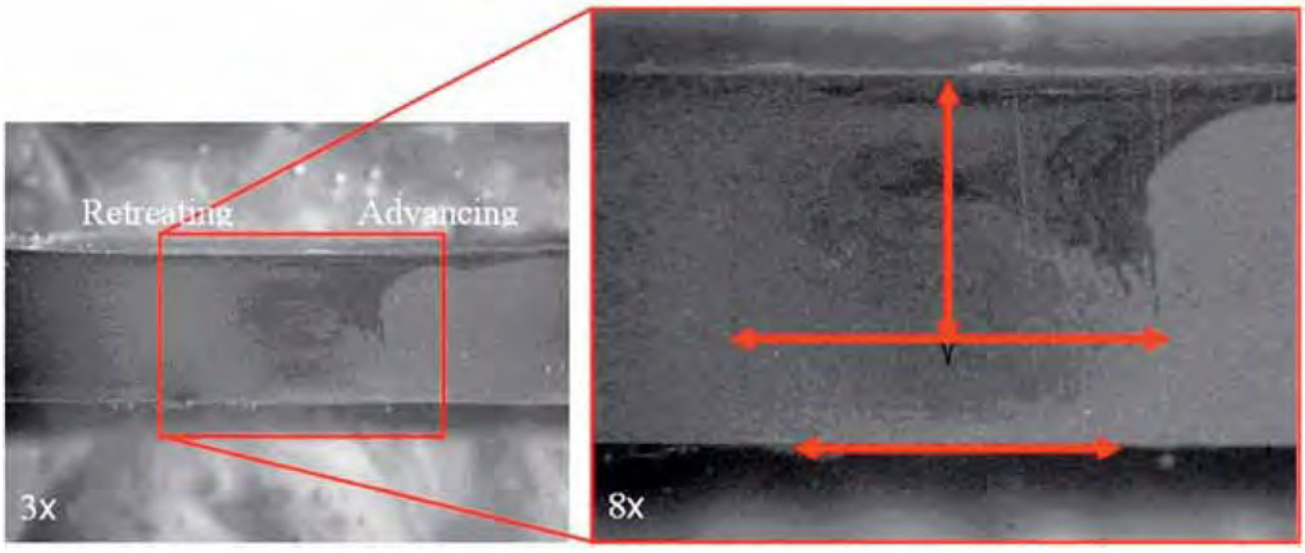

Figure 2 – Photomacrograph of weld welded with striated flat shoulder

Table 2 – Some aspects observed through macrographs

Tool	Position of the centre of the nugget (mm)	Width of nugget at the centre (mm)	Width of nugget at the root (mm)
Smooth concave shoulder	2.2	3.8	3.6
Striated flat shoulder	2.3	3.8	3.6

From the results obtained it is possible to state that the different shoulder geometries investigated do influence the surface finishing and the minimum tilt angle needed for good stability of the process. Nevertheless, they are not relevant in the development and level of penetration of the nugget (not in the vicinity of about 1 mm from the surface in contact with the shoulder), as can be confirmed from the results of Figures 1 and 2 and Table 2.

Thus, the microstructural analysis, presented in Figures 3 to 8 obtained with the smooth concave shoulder, is representative of the results obtained for both shoulder geometries.

Results of the metallurgy analysis can be interpreted by analysing the grain morphology and precipitates density and location:

Figure 3 – Generic identification of micrograph locations

a) Elongated grain
(magnification: X 200. Etching: Poulton's mod.)

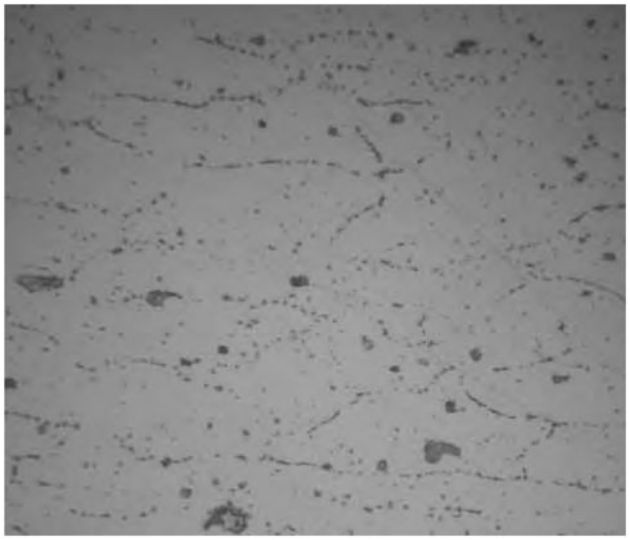

b) Precipitated inter and transgranular
(magnification: X 500. Etching: Fluoridic acid)

Figure 4 – Photomicrograph of parent material (zone a)

a) Elongated grain
(magnification: X 200. Etching: Poulton's mod.)

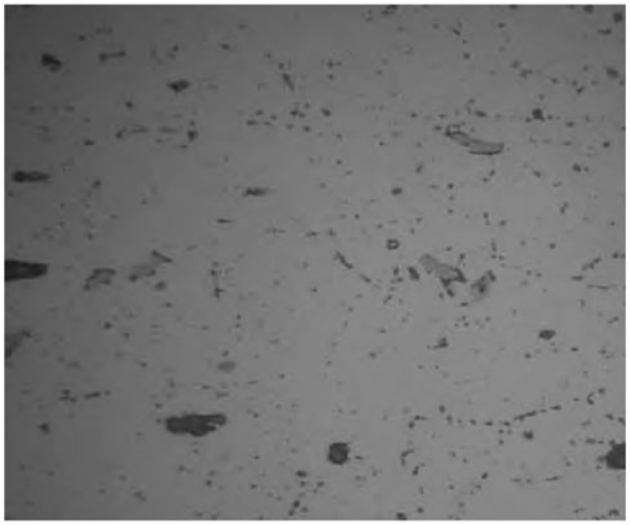

b) Precipitated transgranular
(magnification: X 500. Etching: Fluoridic acid)

Figure 5 – Photomicrograph of HAZ (zone b)

a) Elongated grain plastically deformed (magnification: X 200. Etching: Poulton's mod.)

b) Precipitated transgranular (magnification: X 500. Etching: Fluoridic acid)

Figure 6 – Photomicrograph of TMAZ (zone c)

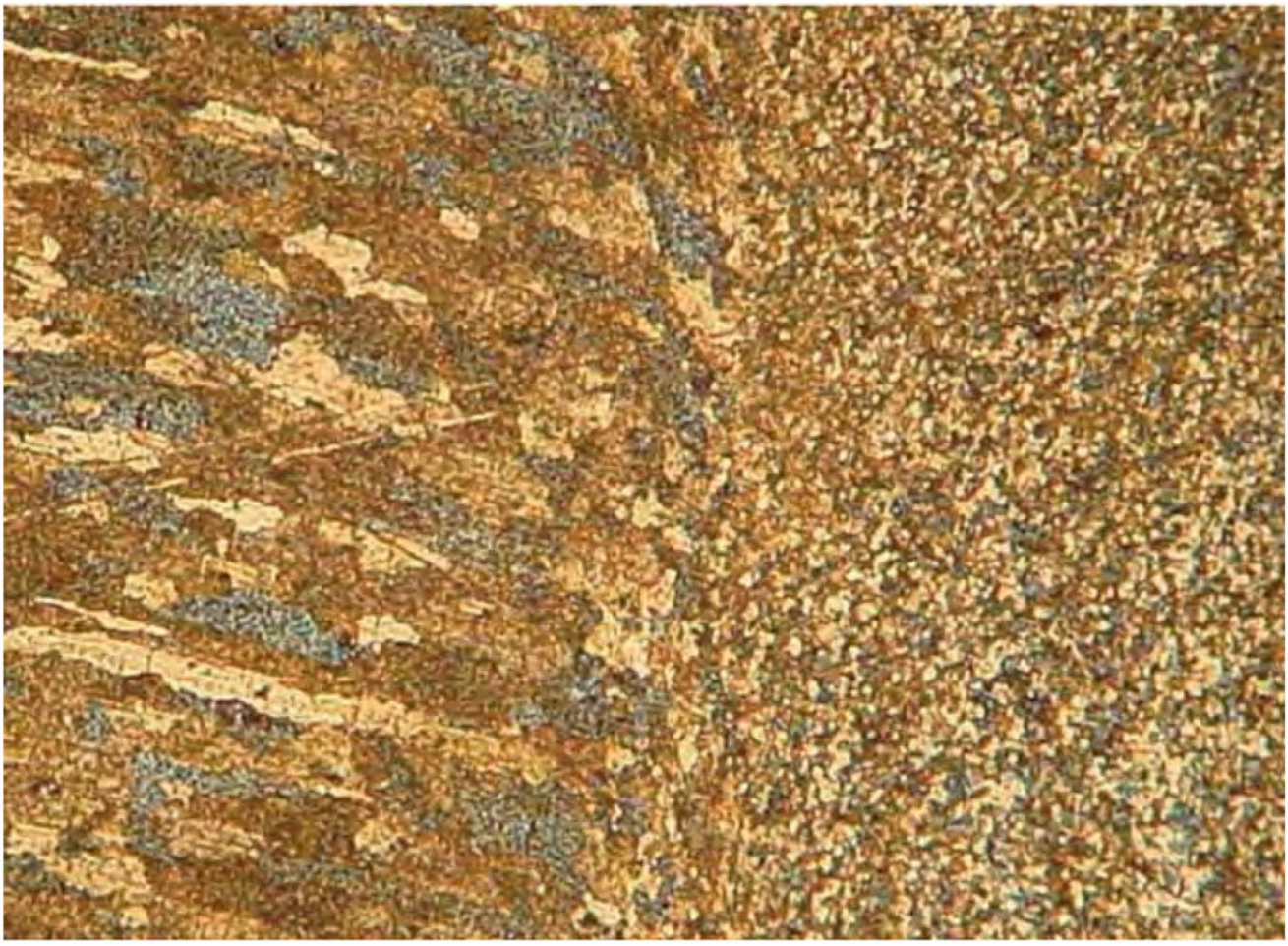

Different grain geometry can be observed (magnification: X 100. Etching: Poulton's mod.)

Figure 7 – Photomicrograph of transition between TMAZ and nugget (zones c and d interface)

– parent material presents elongated grains as result of the original rolling of the plates. Due to the concentration of small precipitates in grain boundaries the grains are well defined. Transgranular precipitates present bigger dimensions than the intergranular precipitates;

– HAZ presents some coalescence of grains. The distribution of precipitates in the grain boundaries is reduced due to dissolution;

– TMAZ grains maintain the characteristics of the HAZ, however the grains present increased deformation as they get close to the interface with the nugget. This fact

a) Equiaxial grain (magnification: X 200. Etching: Poulton's mod.)

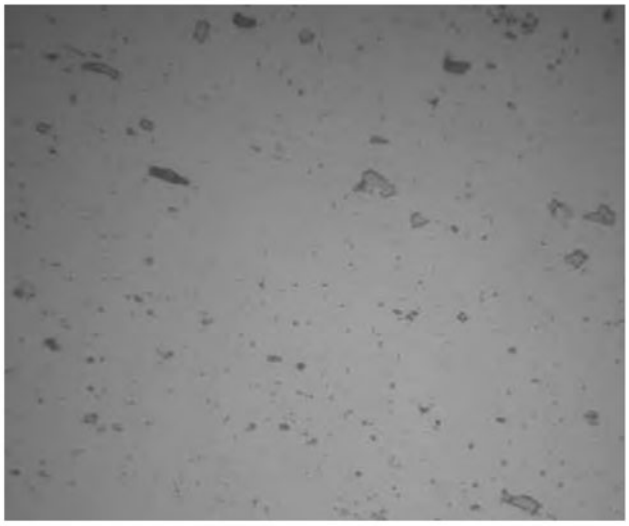

b) Precipitate dispersed in solid solution (magnification: X 500. Etching: Fluoridic acid)

Figure 8 – Photomicrograph of nugget (zone d)

results from the influence of the material flow prescribed by the movement of the tool and the relatively high maximum temperature reached in this zone;
– TMAZ/Nugget interface enhances the significant difference between the structure of the initial grains and the grains resultant from the dynamical recrystallisation process defining the nugget zone;
– Nugget grain is equiaxial, resulting from the dynamical recrystallisation process, presenting a fine dispersion of the precipitates in the solid solution.

3.2 Hardness tests

Vickers hardness tests were performed in order to address some information about the mechanical properties characteristics along the welded zone. The results are presented in Figure 9. From the results obtained, the following comments arise:

– parent material presents an average hardness of 75HV1 and localizes about 13 mm from the centre of the nugget;

– nugget presents an average hardness of 81HV1, about 8 % higher than the parent material, along about 5 mm wide;

– along the TMAZ the hardness decreases from the values of the nugget to the values of the HAZ, with a minimum value of 77HV1, about 5 mm from the nugget centre;

– HAZ starts, at about 5 mm from the nugget centre, and extends for about 6 mm, with an average hardness of 77HV1;

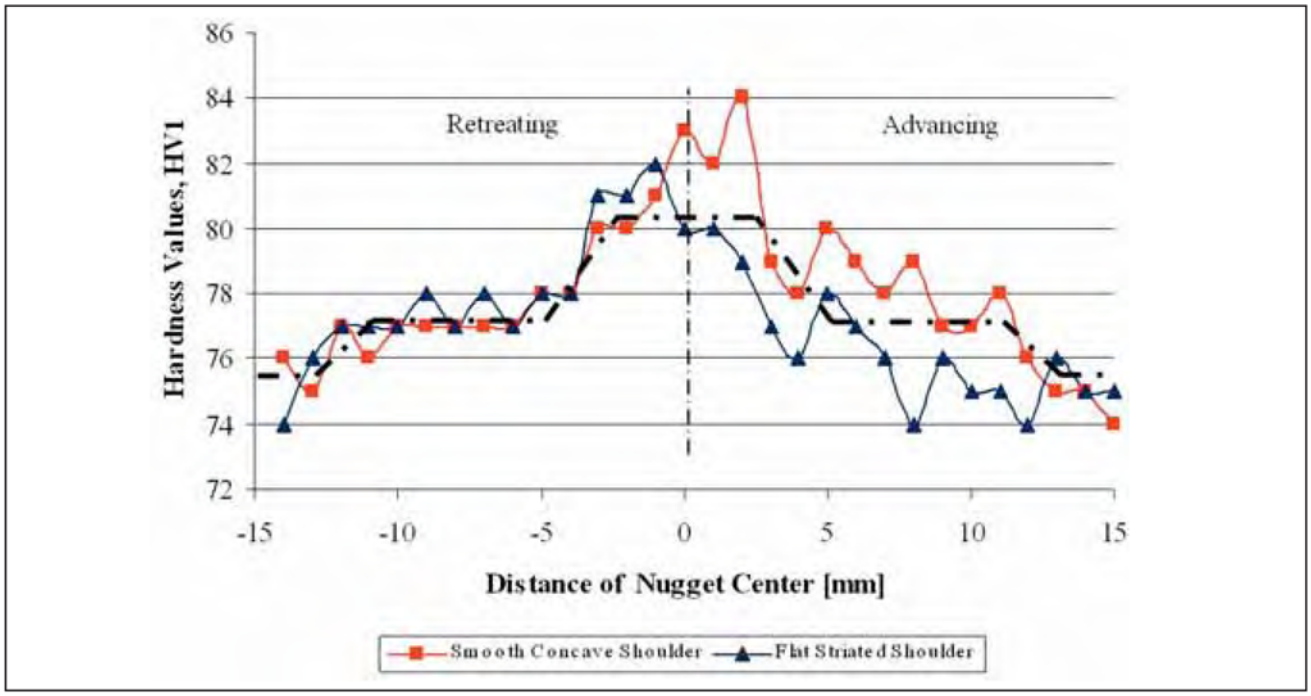

Figure 9 – Vickers hardness tests results with 1 kg of indentation load

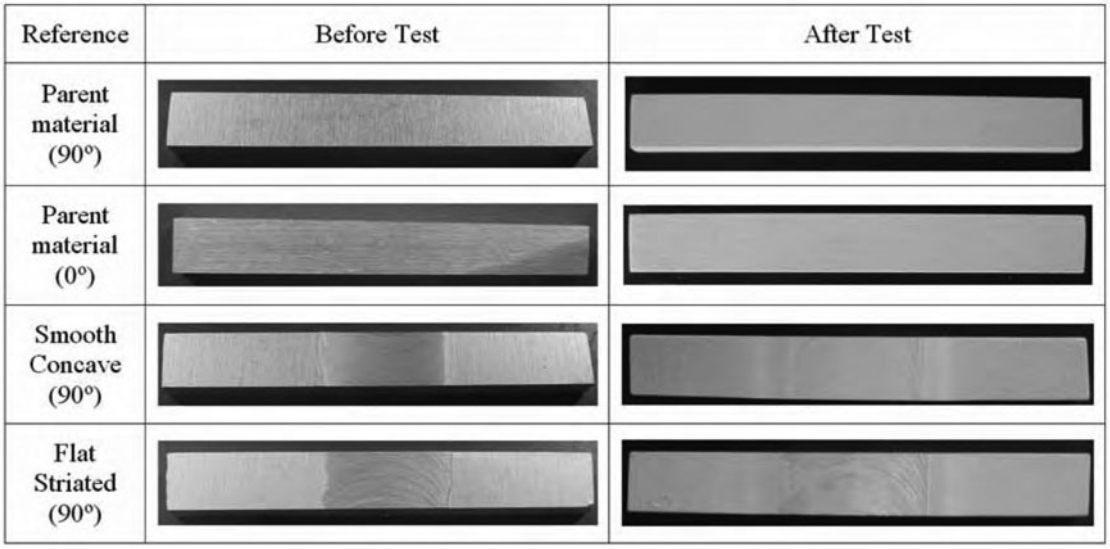

Figure 10 – Samples of parent material and welded plates submitted to intergranular corrosion test, showing results before and after test

– variations of hardness values obtained in different tests of friction stir welding are not significant, as well as differences observed between the advancing and the retreating sides.

3.3 Intergranular corrosion tests

In Figure 10 and Table 3 the results from the intergranular corrosion tests are presented. Figure 10 shows the superficial appearance of both parent materials and welded plates before and after the tests. In the case of parent material, samples are prepared in 0° and 90° directions relative to the original rolling direction.

In Table 3 are established the average and standard deviation results of the loss mass of the parent materials and welded plates resulting from the corrosion tests. In the case of the parent material, samples were prepared in 0° and 90° directions relative to the original rolling direction.

The results of Table 3 allow the following remarks:
– parent material presents a distribution of intergranular precipitates, as shown in the metallographic results, the predominance of the corrosion attack is known to occur in these precipitates [16] and the results obtained emphasize this phenomenon. In fact, the different cutting direction of the parent materials samples, because of the anisotropic structure, results in a higher loss mass for the 90° direction case, where more grain boundaries are exposed and consequently the susceptibility to corrosion is higher;
– the loss mass in the parent material samples is higher than in the welded samples. This result is possible to understand by observing the metallographic analysis. The metallographic results show that in the nugget the grain is smaller and the precipitates are disseminated, and even in the TMAZ and HAZ the concentration of precipitates is less than in the parent material. Thus, the susceptibility to corrosion is reduced in the welded samples;
– between the two welded samples there is a small difference in the loss mass. The corrosion characteristics are similar, showing more intensive corrosion in the parent material zone than in the weld bead. Moreover, the striated zone at the top surface of the welded plates shows a more intense corrosion attack at the retreating side. The existent small difference of loss mass is probably due to the higher susceptibility to corrosion of the plates welded with a smooth concave shoulder, which generates a smoother finishing of the top surface than the striated flat shoulder.

Table 3 – Average and standard deviation results of loss mass of the samples

Samples	Loss mass (mg.cm^{-2})	
	Average value	Standard deviation
Parent material (90°)	22.37	0.02
Parent material (0°)	17.99	1.00
Smooth concave shoulder (90°)	15.54	0.29
Striated flat shoulder (90°)	11.33	0.43

3.4 Exfoliation corrosion tests

In Figure 11 is presented the surface appearance of the samples of parent material and welded plates with the smooth concave shoulder and striated flat shoulder before and after the exfoliation test.

From the analysis of the exfoliation tests of parent material samples, it is possible to verify the occurrence of corrosion in the form of generalized and homogeneously distributed pitting. The same behaviour is obtained in the parent material zone of the welded specimens, but in these cases as it comes near the HAZ the exfoliation is strongly reduced. Although generally less corrosion occurs in the weld zone, the exfoliation in this zone is concentrated at the top surface of the weld bead, at the geometric discontinuity (chip) left by the shoulder action

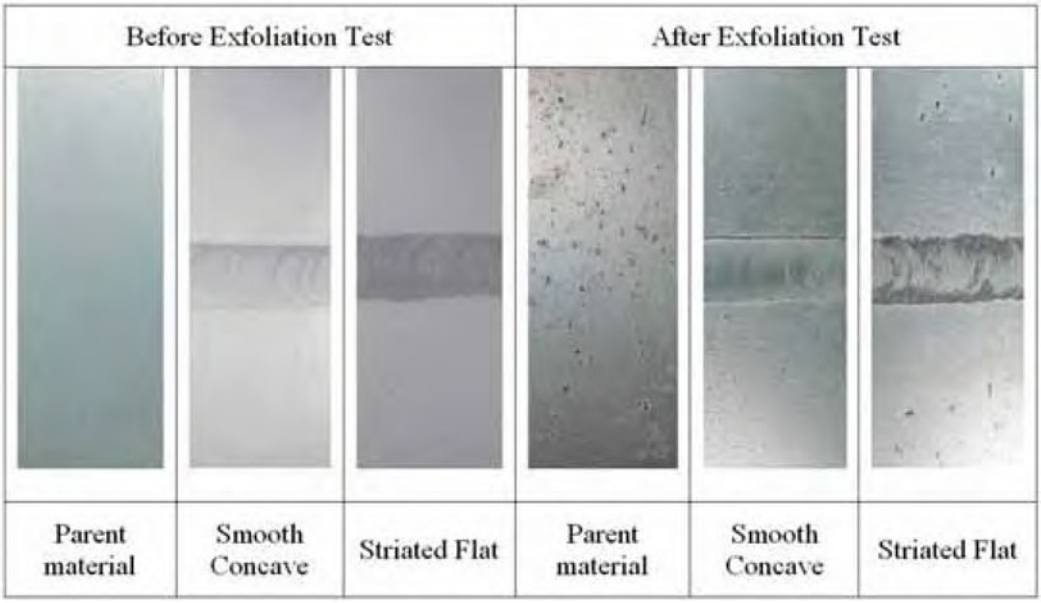

Figure 11 – Samples submitted to exfoliation corrosion test, showing results before and after test

over the original surface of parent material. This fact is probably due to the concentration of the corrosive environment at the chip.

Comparing the two welded conditions, the striated flat shoulder presents more severe corrosion. The highest superficial roughness resulting from the striated flat shoulder action enabled not only the initiation of the corrosion mechanisms, but also the fast propagation through the striate discontinuities. In opposition to this result, the smoother surface finishing result from the smooth concave shoulder does not show any propagation through the striate discontinuities.

3.5 Scanning Electron Microscopy

The SEM observation of the surface of samples before and after corrosion tests allow a better understanding of the previous results.

Figure 12 presents the superficial aspect of the top surface of the parent material and welded zones with a smooth concave shoulder and a striated flat shoulder, prior to the corrosion tests. From Figure 12 a), it is possible to confirm the elongated surface morphology of the parent material resulting from the deformation of the original rolling of the plates. On the other hand, the different surface finishing resulting from the different shoulder geometries shows a smoother surface finishing of the smooth concave shoulder [Figure 12b)] when compared with the result of the striated flat shoulder, which produces a surface finish with larger striates and with a bigger distance between them [Figure 12c)].

After the intergranular corrosion tests, representative photographs of the different zones of the weld sample welded with the smooth concave shoulder are presented in Figure 13. From the photographs of Figure 13 it is observed that the parent material presents a preferential morphology of intergranular attack, while the attack that occurs in the HAZ and weld bead is not so concentrated and less significant.

After the exfoliation corrosion tests, the SEM analysis produced results that are presented in Figure 14. These photographs are representative of the corrosion mechanisms and morphology of the attack occurred in different zones of the welded plates. Pitting morphology of corrosion in the parent material can be observed in Figure 14 a), while Figure 14 b) and 14 c) shows exfoliation attack in the striated zone of the weld with a striated flat shoulder.

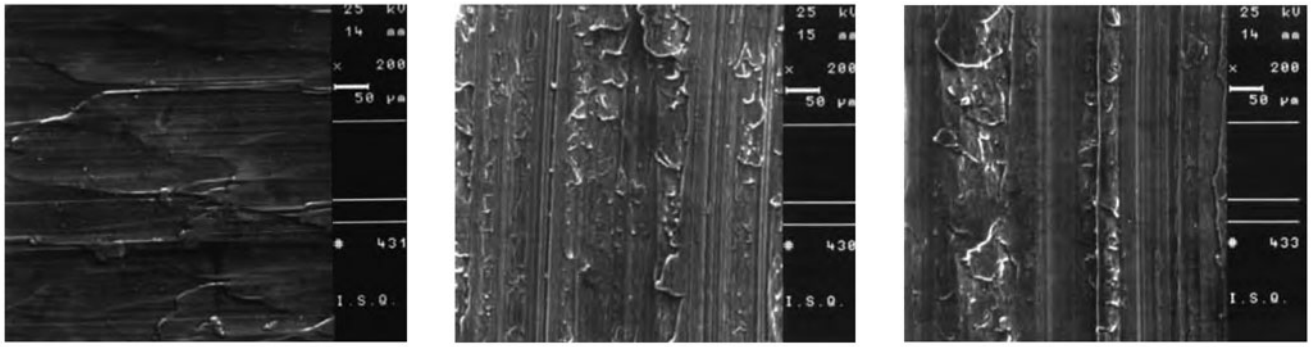

a) Parent material

b) Weld bead welded with smooth concave shoulder

c) Weld bead welded with striated flat shoulder

Figure 12 – Morphology of the top surface before corrosion tests

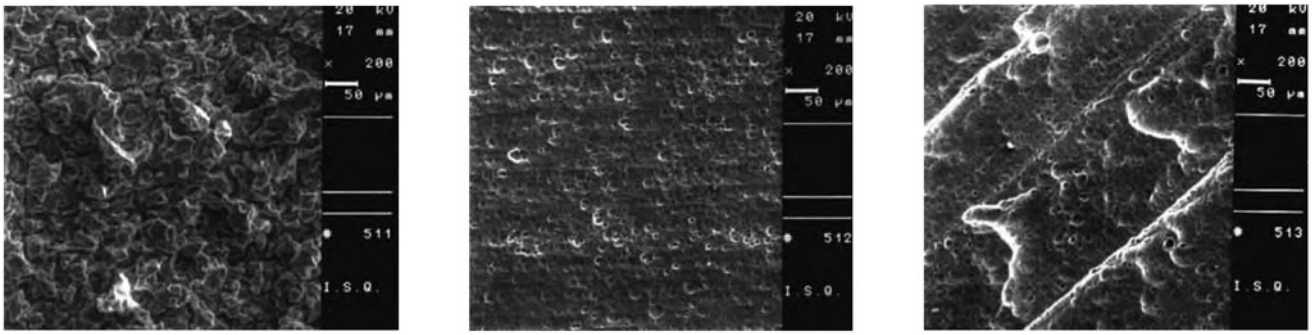

a) Parent material **b) HAZ** **c) Weld bead**

Figure 13 – Morphology of the top surface after intergranular corrosion tests of the welded sample with smooth concave shoulder

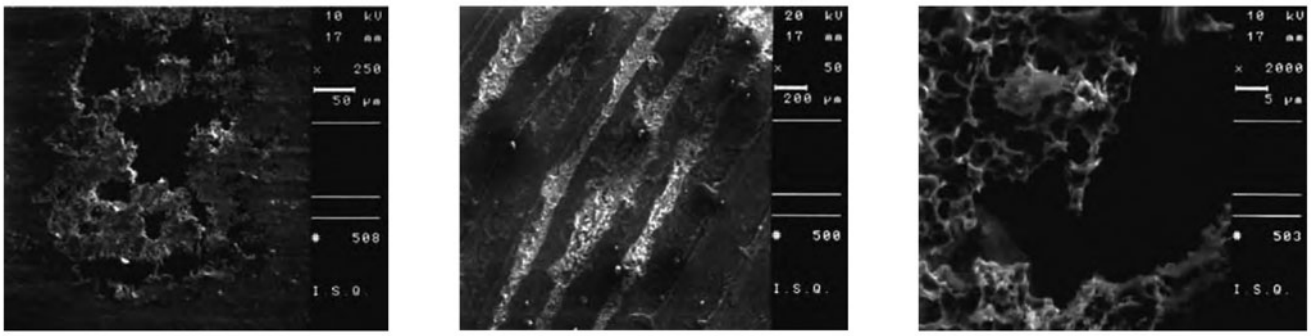

a) Pitting in the parent material **b) Surface exfoliation in the weld bead** **c) Detail of surface exfoliation in the weld bead**

Figure 14 – Morphology of the top surface after exfoliation corrosion tests of the welded sample with smooth concave shoulder

4 CONCLUSIONS

Microstructural evolutions and the hardness profile at mid-thickness do not depend on the modification of the shoulder geometry. For the non-heat treatable aluminium alloy AA5083-H111, the main results from metallographic analysis and hardness tests are the following:
– from the metallographic analysis the emphasis is the small coalescence of grains and the reduction of precipitates in the grain boundaries of the HAZ and TMAZ which play an important role in the prevention of corrosion development;
– the fact that all the weld affected zones present hardness values higher than the parent material allow us to conclude that, at least under static load, the failure would occur in the parent material zone.

The loss mass in the parent material samples is higher than in the welded samples because the intergranular corrosion mechanism is more susceptible at the intergranular precipitates, and these are more abundant in the parent material.

The exfoliation corrosion tests demonstrate that corrosion resistance of the AA5083-H111 is better when welded with the smooth concave shoulder due to better surface finishing of the weld bead. Thus, the higher roughness at the top of the weld bead resulting from the striated flat shoulder promotes the earlier start and faster development of the corrosive attack.

From the SEM analysis it was confirmed that the parent material presents a preferential morphology to intergranular attack, while the attack that occurs in the HAZ and weld bead is not so concentrated and less significant.

ACKNOWLEDGMENTS

The authors would like to acknowledge the financial support from the Fundação para Ciência e Tecnologia (FCT) via the project: POCTI/CTM/41152/01 (acronym iSTIR), and the Estaleiros Navais do Mondego S. A. - Figueira da Foz - Portugal.

REFERENCES

[1] Anderson T.: The advancement of aluminum within the welding fabrication industry and its many product design applications, Alcotec Wire Corporation, USA, 2004.

[2] Facing the future challenges of mobility and competitiveness of Europe, External Advisory Group KA3 Land Transport and Marine Technologies, February 2001.

[3] Svetsaren Esab, The ESAB welding and cutting Journal, Vol. 58 N° 1, 2003.

[4] Anderson T.: New developments within the aluminium shipbuilding industry, Alcotec Wire Corporation, Svetsaren nº 1, 2003.

[5] Kallee S.W.: Friction stir welding – How to weld aluminium without melting it, TWI, London, May 2001.

[6] Larsson H., Karlsson L., Svenson L.: Friction stir welding of AA 5083 and AA 6082 aluminium, Svetsaren, February 2000.

[7] Kallee S.W., Nicholas E.D., Thomas W.M.: Friction stir welding: invention, innovations and industrialisation, Rührreibschweißen (FSW) - Ein modernes Fügeverfahren (Friction welding - A modern joining process), Berlin-Brandenburg, 20 March 2002.

[8] Vilaça P.: Fundamentos do Processo de Soldadura por Fricção Linear – Análise Experimental e Modelação Analítica, PhD Thesis, Instituto Superior Técnico, Universidade Técnica de Lisboa, Setembro 2003.

[9] Thomas W.M., Nicholas E.D., Smith S.D.: Friction stir welding – Tool developments, Aluminum Joining Symposium, 2001 TMS Annual Meeting, 11-15 February 2001, New Orleans, Louisiana, USA.

[10] Jens Klaestrup Kristensen *et al.*: Properties of friction stir welded joints in the aluminium alloys 2024, 5083, 6082/6060 and 7075, 5th International Congress TWI, Metz, 14-16 September 2004.

[11] Mercado U.A., Ghidini T., Dalle Donne C., Braun R.: Fatigue and corrosion properties of friction stir welded dissimilar aluminium alloys; Fifth International Friction Stir Welding Symposium, 14-16 September 2004, Metz, France.

[12] Leonard A.J.: Corrosion resistance of friction stir welds in aluminium alloys 2014A-T651 and 7075-T651, TWI Ltd.

[13] Catarino A., Pépe N., Vilaça P., Quintino L.: Comportamento dos cordões de soldadura por fricção linear na liga de alumínio AA5083 usada na construção naval; Jornadas do Mar, Escola Naval, 2004.

[14] ASTM G67 – Standard test method for determining the susceptibility to intergranular corrosion of 5XXX series aluminium alloys by mass loss after exposure to nitric acid (NAMLT Test), 1999.

[15] ASTM G66 – Standard Test method for visual assessment of exfoliation corrosion susceptibility of 5XXX series aluminium alloys (ASSET Test), 1999.

[16] Polmear I.J.: Light alloys-metallurgy of the light metals, pp. 32, Edward Arnold, 1981.